Modeling Mobility Database Failure Restoration using Checkpoint Schemes

Sok-Ian Sou, *Student Member, IEEE,* and Yi-Bing Lin, *Fellow, IEEE*

***Abstract*— This paper studies checkpointing and failure restoration of mobility database for** *Universal Mobile Telecommunications System* **(UMTS). By utilizing per-user checkpointing technique, individual** *Home Location Register* **(HLR) records are saved into non-volatile backup storage form time to time. When a failure occurs, the backup record is restored back to the mobility database. We consider three per-user checkpoint schemes for the HLR. An analytic model is developed to investigate these schemes in terms of the probability that a HLR backup record is obsolete and the expected checkpoint interval. This model is validated against simulation experiments. Our study provides guidelines for selecting an appropriate checkpoint scheme and parameters for various traffic conditions.**

***Index Terms*— Checkpoint, failure restoration, Home Location Register (HLR), Universal Mobile Telecommunications System (UMTS).**

I. Introduction

THIS paper studies checkpointing and failure restoration of mobility databases for *Universal Mobile Telecommunications System* (UMTS) and *General Packet Radio Service* (GPRS) [2], [9] that support wireless Internet applications. In these networks, the *Home Location Register* (HLR) is a database used for mobile user information management. All permanent subscriber data are stored in this database. An HLR record consists of three types of information: *Mobile Station* (MS) *Information*, *Service Information* and *Location Information*. Both the MS and service information items are only occasionally updated. The location information in the HLR is updated whenever the MS moves to a new *Serving GPRS Support Node* (SGSN). To access the MS, the HLR is queried to identify the current SGSN location of the MS. An MS may move frequently and the location information is often modified. If the HLR fails, the MS will not be accessed by the outside world. To guarantee service availability to the MSs, periodic checkpoint of HLR is mandatory as described in 3GPP TS 23.007 [1]. In this mechanism, the HLR location information is periodically saved into non-volatile backup storage. When an HLR failure occurs, the database recovery procedure is exercised. Several approaches were proposed to checkpoint the HLR database [7]. This paper studies three per-user checkpoint schemes for mobility database failure restoration. We first describe a commonly used checkpoint scheme. Then we discuss two improved checkpoint schemes. An analytic model is developed to compare these three schemes in terms of expected checkpoint interval and the probability that a HLR backup record is obsolete. This analytic model is validated against simulation experiments.

Manuscript received March 22, 2005; revised August 16, 2005 and November 26, 2005; accepted November 27, 2005. The associate editor coordinating the review of this paper and approving it for publication was W. Zhuang.

The authors are with the Department of Computer Science and Information Engineering, National Chiao Tung University, Hsinchu 30010, Taiwan, R.O.C. (e-mail: {sisou, liny}@csie.nctu.edu.tw).

Digital Object Identifier 10.1109/TWC.2007.05200.

II. Per-User Checkpoint Schemes

This section describes three per-user checkpoint schemes. Scheme I is a basic scheme widely used in UMTS checkpointing [3], [4], which is described as follows.

Scheme I. For every MS, this scheme defines a timeout period t_p. When this timer expires, a checkpoint is performed to save the HLR record of the MS into the non-volatile backup storage.

Both Schemes II and III take delayed registration approach with the following intuition. Suppose that after a checkpoint is performed, no registration has occurred before the t_p timer expires. In this situation, there is no need to checkpoint the record because the backup copy is still valid. Details of Schemes II and III are described as follows.

Scheme II [7]. If no registration has occurred before the t_p timer expires, the backup record is the same as that in the HLR. Therefore, checkpoint is postponed until the next registration occurs. To implement Scheme II, a tri-state *Finite State Machine* (FSM) is implemented for every HLR record (see Fig. 1 (a)). **State 0** represents that neither registration event nor t_p timeout event occurs after the previous checkpoint. **State 1** represents that after the previous checkpoint, the first registration event occurs before a t_p timeout event does. Note that the backup record is obsolete in this state. **State 2** represents that after the previous checkpoint, a t_p timeout event occurs before a registration event does. Initially, the FSM is in **State 0**, and the t_p timer starts to decrement. If a registration event occurs before the t_p timer expires, the FSM moves to **State 1**, and remains in **State 1** until the t_p timeout event occurs. At this point, the HLR record is checkpointed into the backup, the t_p timer is restarted, and the FSM moves back to **State 0**. If the timeout event occurs at **State 0**, the FSM moves to **State 2** and the t_p timer is stopped. If a registration event occurs at **State 2**, a checkpoint is performed, the t_p timer is restarted, and the FSM moves back to **State 0**.

Scheme III. Scheme III is the same as Scheme I except that Scheme III will check whether a registration has occurred when the t_p timer expires. If no registration occurs, the backup record is valid, then Scheme III simply restarts the t_p timer without checkpointing the record. In this scheme, a two-state FSM is implemented for every HLR record

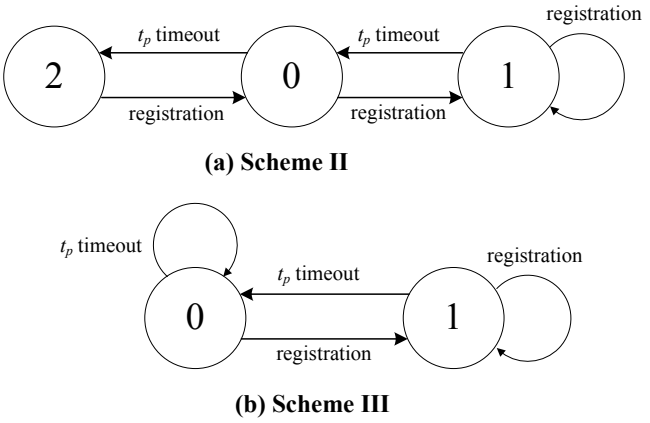

Fig. 1. State diagrams for schemes II and III.

(see Fig. 1 (b)). **State 0** represents that no registration occurs after the previous checkpoint. **State 1** represents that a registration occurs after the previous checkpoint. Note that the backup record is obsolete in this state. Initially, the FSM is in **State 0**, and the t_p timer starts to decrement. If a registration event occurs, the FSM moves to **State 1** and remains in **State 1** until the t_p timeout event occurs. Then the FSM moves back to **State 0**, the HLR record is checkpointed into the backup, and the t_p timer is restarted. If the timeout event occurs at **State 0**, it means that no registration event has occurred after the previous checkpoint. The t_p timer is restarted and the FSM keeps staying in **State 0** without performing any checkpoint.

In the subsequent sections, we investigate the performance of Schemes I, II and III by considering two output measures, the probability of obsolete HLR record α and the expected checkpoint interval $E[t_c]$.

III. Analytic Model for Exponential t_p Timer

In a typical checkpoint approach, fixed t_p is selected. Since we consider per-user checkpointing, fixed t_p may result in a large number of simultaneous checkpoints that cause congestion. In such case, one may select exponential timeout t_p with mean $1/\lambda$ and the density function

$$f_p(t_p) = \lambda e^{-\lambda t_p} \tag{1}$$

Exponential checkpoint intervals are widely used to resolve access backoff problems [10]. As we shall see in Section V, fixed t_p yields better performance than exponential t_p in some cases, and exponential t_p outperforms fixed t_p in other cases. In this section, we consider exponential t_p for Schemes I, II and III. In the next section, we consider analytic analysis with fixed t_p for Schemes I and III.

Let random variable t_m denote the inter-registration time, which has an arbitrary density function $f_m(t_m)$, the mean $1/\mu_m$ and the Laplace transform $f_m^*(s) = \int_{t_m=0}^{\infty} f_m(t_m)e^{-st_m}dt_m$. Two output measures are considered for checkpoint performance:

- α: the probability that the HLR record in the backup is obsolete when a failure occurs. The smaller the α value, the better the checkpoint performance. We use α_i to represent the α value for Scheme i ($i = I, II$ or III).
- $E[t_c]$: the expected checkpoint interval. The larger the $E[t_c]$ value, the lower the checkpoint overhead. We use $E_i[t_c]$ to represent the $E[t_c]$ value for Scheme i ($i = I, II$ or III).

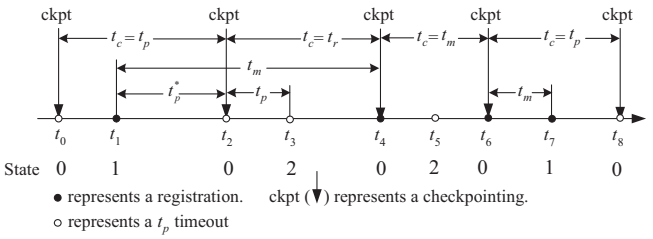

Fig. 2. Timing diagram for scheme II.

The analytic models developed in this and the next sections are validated against simulation experiments. The details will be given in Section V.

A. Modeling of Schemes I and II

In [7], an analytic model was proposed for Schemes I and II. For Scheme I, α_I and $E_I[t_c]$ were derived as

$$\alpha_I = \left(\frac{\mu_m}{\lambda}\right)[1 - f_m^*(\lambda)] \quad \text{and} \quad E_I[t_c] = \frac{1}{\lambda} \tag{2}$$

In the analytic analysis of Scheme II in [7], the arrival of a registration event is considered as a random observer of the inter-checkpoint arrival times. This random observer assumption is accurate if the inter-registration times are exponentially distributed. However, when the inter-registration times have an arbitrary distribution with large variance, the random observer assumption may cause inaccuracy in deriving α_{II} and $E_{II}[t_c]$. In this paper, a new approach is proposed to accurately compute α_{II} and $E_{II}[t_c]$.

To describe the notation used in our derivation, consider the timing diagram in Fig. 2. At time t_0, the FSM is at **State 0** (when a t_p timeout occurs). At time t_1, the next registration occurs and the FSM moves from **State 0** to **State 1**. At time t_2, the t_p timer expires and the FSM moves from **State 1** to **State 0**. The checkpoint interval $t_c = t_2 - t_0$ is equal to t_p. Let $t_p^* = t_2 - t_1$. From the memoryless property, t_p^* has the same distribution as t_p. At time t_3, the t_p timer expires again and the FSM moves from **State 0** to **State 2**. At time t_4, a registration occurs (where $t_m = t_4 - t_1$ is the inter-registration interval). The FSM moves from **State 2** to **State 0**, and $t_c = t_4 - t_2 = t_r$. In [7], t_r was modeled as the residual time of t_m. Since the checkpoint time t_2 may not be a random observer of t_m periods, inaccuracy may be incurred. The exact density function $f_r(t_r)$ for t_r is derived as follows. As shown in Fig. 2, $t_r = t_4 - t_2$ can be written as $t_r = (t_4 - t_1) - (t_2 - t_1) = t_m - t_p^*$ where $t_m > t_p^*$. That is, t_r can be represented by the difference of two random variables t_m and t_p^* under the condition that $t_m > t_p^*$. Therefore, the density

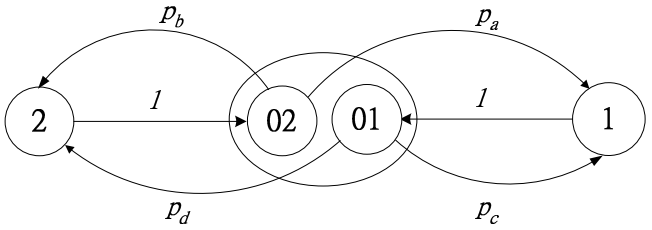

Fig. 3. Modified state diagram for scheme II.

function $f_r(t_r)$ is computed as a conditional probability

$$\begin{aligned} f_r(t)dt &= \frac{\Pr[t < t_m - t_p^* < t + dt \text{ and } t_m > t_p^*]}{\Pr[t_m > t_p^*]} \\ &= \frac{\int_{t_p^*=0}^{\infty} f_m(t + t_p^*)dt f_p(t_p^*)dt_p^*}{\int_{t_p^*=0}^{\infty}\int_{t_m=t_p^*}^{\infty} f_m(t_m)dt_m f_p(t_p^*)dt_p^*} \\ &= \frac{\int_{t_p^*=0}^{\infty} f_m(t + t_p^*)e^{-\lambda t_p^*}dt_p^* dt}{\int_{t_p^*=0}^{\infty}\int_{t_m=t_p^*}^{\infty} f_m(t_m)dt_m e^{-\lambda t_p^*}dt_p^*} \end{aligned} \quad (3)$$

When t_m has the η-Erlang distribution with the shape parameter η and the scale parameter $\eta\mu_m$ (i.e., the mean is $1/\mu_m$), it has the density function

$$f_m(t_m) = \left[\frac{(\eta\mu_m t_m)^{\eta-1}}{(\eta-1)!}\right]\eta\mu_m e^{-\eta\mu_m t_m} \quad (4)$$

From (4), (3) is re-written as

$$\begin{aligned} f_r(t_r) &= \left[\sum_{j=0}^{\eta-1}\left(\frac{\eta\mu_m}{\eta\mu_m+\lambda}\right)^j\right]^{-1}\left[\frac{(\eta\mu_m)^\eta e^{-\eta\mu_m t_r}}{(\eta-1)!}\right] \\ &\quad\times\sum_{k=0}^{\eta-1}\binom{\eta-1}{k}t_r^{\eta-1-k}k!\left(\frac{1}{\eta\mu_m+\lambda}\right)^k \end{aligned} \quad (5)$$

When t_m is exponentially distributed (i.e., $\eta = 1$), (5) is simplified as $f_r(t_r) = \mu_m e^{-\mu_m t_r}$. This result is consistent with the memoryless property for exponential t_m distribution. In Scheme II, if the t_p timer is restarted due to the t_p timeout event (i.e., a transition from **State 1** to **State 0**; see t_2 in Fig. 2), then the next checkpoint interval is $t_c = \max(t_p, t_r)$. On the other hand, if the t_p timer is restarted due to a registration event (i.e., a transition from **State 2** to **State 0**; see t_6 in Fig. 2), then the next checkpoint interval is $t_c = \max(t_m, t_p)$. To distinguish the above two cases, **State 0** in Fig. 1 (a) is split into **State 01** and **State 02**.

Fig. 3 draws the modified state diagram for Scheme II. If a checkpoint occurs due to a t_p timeout event, then the FSM moves from **State 1** to **State 01**. If a checkpoint occurs due to a registration event, then the FSM moves from **State 2** to **State 02**. Detailed derivation for $E_{II}[t_c]$ was given in [7]. For the reader's benefit, we summarize the derivation here. Let π_x be the stationary probability that the FSM is in **State x**. Let p_1 and p_2 represent the conditional probabilities that if the FSM is in **State 0**, it is in **State 01** and **State 02**, respectively. That is,

$$p_1 = \frac{\pi_{01}}{\pi_{01}+\pi_{02}} \quad \text{and} \quad p_2 = \frac{\pi_{02}}{\pi_{01}+\pi_{02}} \quad (6)$$

In Fig. 3, the transition probabilities from **State 02** to **State 1** and **State 2** are p_a and p_b, respectively. The transition probabilities from **State 01** to **State 1** and **State 2** are p_c and p_d, respectively. In [7], the above probabilities were derived as

$$\left.\begin{aligned} p_a = f_m^*(\lambda) \quad , \quad p_b = 1 - f_m^*(\lambda) \\ p_c = f_r^*(\lambda) \quad , \quad p_d = 1 - f_r^*(\lambda) \end{aligned}\right\} \quad (7)$$

where $f_r^*(\lambda)$ can be derived from (3) using the definition of Laplace Transform. From (7), we can derive π_{01} and π_{02} as

$$\left.\begin{aligned} \pi_{01} = \frac{f_m^*(\lambda)}{2[1+f_m^*(\lambda)-f_r^*(\lambda)]} \\ \pi_{02} = \frac{1-f_r^*(\lambda)}{2[1+f_m^*(\lambda)-f_r^*(\lambda)]} \end{aligned}\right\} \quad (8)$$

and then from (6) and (8) we have

$$p_1 = \frac{f_m^*(\lambda)}{1+f_m^*(\lambda)-f_r^*(\lambda)} \quad , \quad p_2 = \frac{1-f_r^*(\lambda)}{1+f_m^*(\lambda)-f_r^*(\lambda)} \quad (9)$$

From (1), (3) and (9), the expected checkpoint interval $E_{II}[t_c]$ is derived as

$$\begin{aligned} E_{II}[t_c] &= p_1 E[\max(t_p, t_r)] + p_2 E[\max(t_m, t_p)] \\ &= p_1\left\{\frac{f_r^*(\lambda)}{\lambda} + E[t_r]\right\} + p_2\left\{\frac{f_m^*(\lambda)}{\lambda} + \frac{1}{\mu_m}\right\} \end{aligned} \quad (10)$$

where $E[t_r] = \int_{t_r=0}^{\infty} t_r f_r(t_r)dt_r$.

Accurate α_{II} probability is derived in this paper as follows. We first note that the HLR backup record is obsolete only when the FSM is in **State 1**. Since a failure is considered as a random observer of the checkpoint intervals, probability α_{II} can be computed as the proportion of time that the FSM is in **State 1** in the checkpoint interval. In Fig. 2, the FSM is in **State 0** after a checkpoint. There are two possibilities for the first event occurring in the checkpoint interval.

Case I. After the previous checkpoint, the first event is a registration event (with probability $p_1p_c + p_2p_a$). In this case, the FSM moves to **State 1** (see t_1 and t_7 in Fig. 2). The FSM stays in **State 1** until the t_p timer expires (see t_2 and t_8 in Fig. 2). From the memoryless property, the periods that the FSM stay in **State 1** (i.e., $t_2 - t_1$ and $t_8 - t_7$ in Fig. 2) have the same distribution as t_p. Therefore, the expected value that the FSM stays in **State 1** is $1/\lambda$.

Case II. After the previous checkpoint, the first event is a t_p timeout event (with probability $p_1p_d + p_2p_b$). In this case, the FSM moves to **State 2** (see t_3 and t_5 in Fig. 2). The FSM stays in **State 2** until a registration event occurs (see t_4 and t_6 in Fig. 2). Since the FSM does not visit **State 1**, the expected value that the FSM stays in **State 1** is 0.

Therefore, α_{II} can be expressed as

$$\begin{aligned} \alpha_{II} &= \frac{E[\text{time spent in } \textbf{State 1} \text{ in the checkpoint interval}]}{E[\text{checkpoint interval}]} \\ &= \frac{(p_1p_c + p_2p_a)(1/\lambda) + (p_1p_d + p_2p_b)\times 0}{E_{II}[t_c]} \quad (11) \\ &= \frac{(p_1p_c + p_2p_a)(1/\lambda)}{E_{II}[t_c]} \quad (12) \end{aligned}$$

In (11), the first term represents the situation when Case I holds and the second term represents the situation when Case II holds. From (7) and (9), (12) is re-written as

$$\begin{aligned}\alpha_{II} &= \left\{\frac{f_m^*(\lambda)f_r^*(\lambda)}{1+f_m^*(\lambda)-f_r^*(\lambda)}+\frac{[1-f_r^*(\lambda)]f_m^*(\lambda)}{1+f_m^*(\lambda)-f_r^*(\lambda)}\right\} \\ &\quad\times\left(\frac{1}{\lambda E_{II}[t_c]}\right) \\ &= \left[\frac{f_m^*(\lambda)}{1+f_m^*(\lambda)-f_r^*(\lambda)}\right]\left(\frac{1}{\lambda E_{II}[t_c]}\right) \qquad (13)\end{aligned}$$

B. Modeling of Scheme III

This subsection derives the output measures of Scheme III. Based on the description for Scheme III in Section II, it is clear that the α performance in both Schemes I and III are the same. From (2), we have

$$\alpha_{III}=\left(\frac{\mu_m}{\lambda}\right)[1-f_m^*(\lambda)] \qquad (14)$$

The output measure $E_{III}[t_c]$ is derived as follows. The probability that the backup record is obsolete when a t_p timeout event occurs is equal to α_{III}. When the t_p timer expires, the checkpoint is not performed with probability $1-\alpha_{III}$. Therefore, the number of t_p timeouts occurring in an checkpoint interval has a geometric distribution. From (1) and (14), $E_{III}[t_c]$ can be expressed as

$$\begin{aligned}E_{III}[t_c] &= \left[\sum_{n=1}^{\infty} n(1-\alpha_{III})^{n-1}\alpha_{III}\right]E[t_p] \\ &= \frac{1}{\mu_m[1-f_m^*(\lambda)]} \qquad (15)\end{aligned}$$

IV. Analytic Model for Schemes I and III with Fixed t_p Timer

In this section, we present the analytic model for fixed t_p timer with value $1/\lambda$ in Schemes I and III. It is clear that $E_I[t_c]=1/\lambda$, which is the same as that for the exponential t_p case. Consider the timing diagram in Fig. 4 (a). Let τ_p be the interval between the previous t_p timeout and when the failure occurs. Since the failure can be considered as a random observer of the t_p intervals, τ_p is uniformly distributed over $[0,1/\lambda]$. Let τ_a be the interval between when the previous registration occurs and when the failure occurs; in other words, τ_a is the reverse residual time of t_m. According to the reverse residual time theorem [6], τ_a has the same distribution as the residual time of t_m. That is, τ_a has the density function

$$r_m(\tau_a)=\frac{1-\int_{t=0}^{\tau_a}f_m(t)dt}{E[t_m]}=\mu_m\left[1-\int_{t=0}^{\tau_a}f_m(t)dt\right] \qquad (16)$$

In Fig. 4 (a), the HLR backup record is obsolete if $\tau_p>\tau_a$. Therefore, the probability that the HLR backup is obsolete when a failure occurs in Schemes I and III is derived as

$$\alpha_I=\alpha_{III}=\Pr[\tau_p>\tau_a]=\lambda\int_{\tau_p=0}^{1/\lambda}\int_{\tau_a=0}^{\tau_p}r_m(\tau_a)d\tau_a d\tau_p \qquad (17)$$

Substitute (16) into (17), we have

$$\begin{aligned}\alpha_I &= \alpha_{III} \\ &= \lambda\mu_m\int_{\tau_p=0}^{1/\lambda}\int_{\tau_a=0}^{\tau_p}\left[1-\int_{t=0}^{\tau_a}f_m(t)dt\right]d\tau_a d\tau_p \qquad (18)\end{aligned}$$

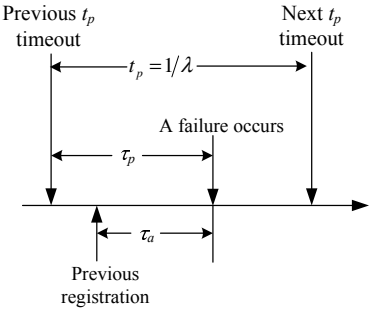

(a) Timing diagram for deriving α_I and α_{III}

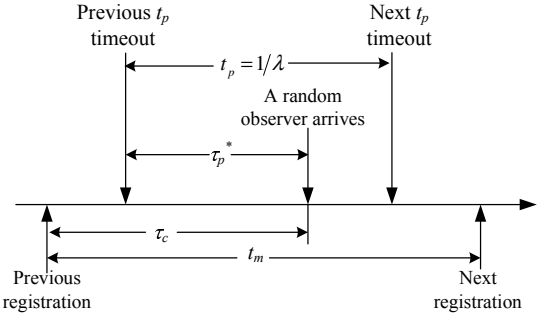

(b) Timing diagram for deriving β

Fig. 4. Timing diagram for schemes I and III (fixed t_p).

To compute $E_{III}[t_c]$, we first derive the probability β that a checkpoint is not performed when the next t_p timer expires. Consider the timing diagram in Fig. 4 (b), where a random observer falls into two consecutive t_p timeouts. Let τ_p^* be the interval between the previous t_p timeout and when the random observer arrives. Then τ_p^* is uniformly distributed over $[0,1/\lambda]$. Let t_m be the inter-registration interval and τ_c be the interval between when the previous registration occurs and when the random observer arrives. It is clear that τ_c has the same distribution as τ_a. If $\tau_c>\tau_p^*$, there is no registration occurs between the previous t_p timeout and when the random observer arrives. Note that $t_m>\tau_c$ in this case. On the other hand, if $t_m>\frac{1}{\lambda}+\tau_c-\tau_p^*$, there is no registration occurs in period between when the random observer arrives and when the next t_p timeout occurs. Therefore, the probability β that there is no registration occurs between two consecutive t_p timeouts can be derived as

$$\begin{aligned}\beta &= \Pr[\tau_c>\tau_p^* \quad\text{and}\quad t_m>(\frac{1}{\lambda}+\tau_c-\tau_p^*)|t_m>\tau_c] \\ &= \lambda\int_{\tau_p^*=0}^{1/\lambda}\int_{\tau_c=\tau_p^*}^{\infty}r_m(\tau_c) \\ &\quad\times\int_{t_m=\frac{1}{\lambda}+\tau_c-\tau_p^*}^{\infty}\frac{f_m(t_m)}{[1-\int_{t=0}^{\tau_c}f_m(t)dt]}dt_m d\tau_c d\tau_p^* \qquad (19)\end{aligned}$$

Substitute (16) into (19) to yield

$$\beta=\lambda\mu_m\int_{\tau_p^*=0}^{1/\lambda}\int_{\tau_c=\tau_p^*}^{\infty}\int_{t_m=1/\lambda+\tau_c-\tau_p^*}^{\infty}f_m(t_m)dt_m d\tau_c d\tau_p^* \qquad (20)$$

When the t_p timer expires, the checkpoint is not performed with probability β. Therefore, the number of t_p timeouts occurring in an checkpoint interval has a geometric distribution.

The expected checkpoint interval $E_{III}[t_c]$ can be derived as

$$E_{III}[t_c] = \left[\sum_{n=1}^{\infty} n\beta^{n-1}(1-\beta)\right] E[t_p] = \frac{1}{(1-\beta)\lambda} \quad (21)$$

where β can be obtained from (20).

For the illustration purposes, we assume that t_m has a 2-Erlang distribution with mean $1/\mu_m$ and Laplace Transform

$$f_m^*(s) = \left(\frac{2\mu_m}{2\mu_m + s}\right)^2 \quad (22)$$

A more general t_m distribution will be considered by simulation experiments later. From (5), $f_r(t_r)$ is expressed as

$$f_r(t_r) = \left(\frac{2\mu_m + \lambda}{4\mu_m + \lambda}\right)\left(t_r + \frac{1}{2\mu_m + \lambda}\right) 4{\mu_m}^2 e^{-2\mu_m t_r} \quad (23)$$

From (23) and the definition of the Laplace Transform, we have

$$f_r^*(\lambda) = \frac{8{\mu_m}^2}{(4\mu_m + \lambda)(2\mu_m + \lambda)} \quad (24)$$

For Scheme I, $E_I[t_c]$ is expressed in (1), which is not affected by the t_m distribution. From (2), (14) and (22), the obsolete HLR backup probabilities for Schemes I and III are

$$\alpha_I = \alpha_{III} = \frac{\mu_m(4\mu_m + \lambda)}{(2\mu_m + \lambda)^2} \quad (25)$$

From (9), (10), (22) and (24), the expected checkpoint interval for Scheme II is

$$\begin{aligned} E_{II}[t_c] &= \frac{p_1}{(4\mu_m + \lambda)}\left[\frac{8{\mu_m}^2}{\lambda(2\mu_m + \lambda)} + \frac{\lambda}{\mu_m} + 3\right] \\ &\quad + (1 - p_1)\left[\frac{1}{\lambda}\left(\frac{2\mu_m}{2\mu_m + \lambda}\right)^2 + \frac{1}{\mu_m}\right] \end{aligned} \quad (26)$$

where from (9), (22) and (24),

$$p_1 = \frac{4{\mu_m}^2(4\mu_m + \lambda)}{(2\mu_m + \lambda)^2(4\mu_m + \lambda) - 4{\mu_m}^2\lambda} \quad (27)$$

From (13), (22) ,(24) and (26), the obsolete HLR backup probability for Scheme II is

$$\alpha_{II} = \left[\frac{4{\mu_m}^2(4\mu_m + \lambda)}{(2\mu_m + \lambda)^2(4\mu_m + \lambda) - 4{\mu_m}^2\lambda}\right]\left(\frac{1}{\lambda E_{II}[t_c]}\right) \quad (28)$$

From (15) and (22), the checkpoint interval for Scheme III is

$$E_{III}[t_c] = \frac{(2\mu_m + \lambda)^2}{\mu_m\lambda(4\mu_m + \lambda)} \quad (29)$$

Equations (25)-(29) have been validated against the simulation experiments. The simulation model follows the discrete event approach in [8], and the details are omitted.

V. Numerical Examples

This section uses numerical examples to investigate the performance of the three checkpoint schemes. Based on the analytic models proposed in Sections III and IV, we compute the output measures α and $E[t_c]$ of the three checkpoint schemes.

Effects of Schemes I, II and III with exponential t_p timer. Fig. 5 plots the output measures α and $E[t_c]$ against λ.

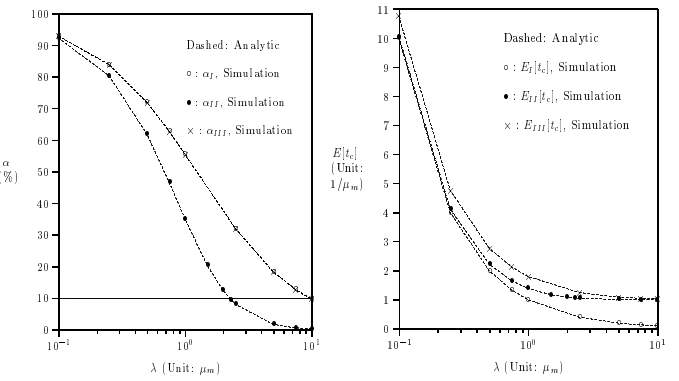

Fig. 5. Effects of λ on α and $E[t_c]$ (exponential t_p).

In this figure, the dashed curves are for analytic results. The $\circ$, $\bullet$ and $\times$ points represent simulation data. This figure shows that the analytic and simulation models are consistent (the errors are within 0.3%). Fig. 5 shows the trivial phenomenon that both α and $E[t_c]$ decrease when λ increases. The non-trivial result is that Fig. 5 quantitatively indicates how to choose λ value to ensure that the α value is under a predefined threshold set by the mobile operator. For example, if the mobile operator requires that the α value be less than 10%, then we should choose $\lambda = 2.3\mu_m$ in Scheme II and $\lambda = 10\mu_m$ in both Schemes I and III (see the horizonal line in the α part of Fig. 5). We also observe that both Schemes II and III are better than Scheme I in terms of the α and the $E[t_c]$ performance. Scheme II is always better than Scheme III in terms of α, and Scheme III is always better than Scheme II in terms of $E[t_c]$.

Effects of exponential and fixed t_p. We consider both exponential and fixed t_p timers with the same means $1/\lambda$. If t_m has a 2-Erlang distribution, then from (18), the probability of obsolete HLR backup record with fixed t_p timer is computed as

$$\begin{aligned} \alpha_I &= \alpha_{III} \\ &= \lambda\mu_m \int_{\tau_p=0}^{\frac{1}{\lambda}} \int_{\tau_a=0}^{\tau_p} \\ &\quad (e^{-2\mu_m\tau_a} + 2\mu_m\tau_a e^{-2\mu_m\tau_a}) d\tau_a d\tau_p \\ &= 1 - \frac{3\lambda}{4\mu_m} + \left(\frac{1}{2} + \frac{3\lambda}{4\mu_m}\right) e^{-2\mu_m/\lambda} \end{aligned} \quad (30)$$

From (20) and (21), the expected checkpoint interval with fixed t_p timer for Scheme III is computed as

$$E_{III}[t_c] = \left\{\lambda\left[1 - \left(\frac{1}{\mu_m} + \frac{1}{\lambda}\right) e^{-2\mu_m/\lambda}\right]\right\}^{-1} \quad (31)$$

Both (30) and (31) are validated against the discrete event simulation model where the errors between the simulation data and analytic data are within 0.2%. Therefore, our models for fixed t_p are correct.

We investigate the effects of exponential and fixed t_p timers by two indicators. Let indicator I_α represent the percentage of reduction for α provided by fixed t_p over

TABLE I
COMPARISON OF EXPONENTIAL t_p TIMER AND FIXED t_p TIMER ON α

	Scheme I			**Scheme II**			**Scheme III**		
λ (Unit: μ_m)	Exponential $t_p(\%)$	Fixed $t_p(\%)$	I_α	Exponential $t_p(\%)$	Fixed $t_p(\%)$	I_α	Exponential $t_p(\%)$	Fixed $t_p(\%)$	I_α
0.1	92.9700	92.5000	0.51%	92.3000	92.4966	-0.21%	92.9700	92.5000	0.51%
0.25	83.9500	81.2500	3.22%	80.4600	81.2412	-0.97%	83.9500	81.2500	3.22%
0.5	72.0000	64.1100	10.96%	61.9400	61.9338	0.01%	72.0000	64.0900	10.99%
0.75	62.8100	51.1200	18.61%	46.6900	43.2917	7.28%	62.8100	51.0900	18.66%
1	55.5600	41.8800	24.62%	35.0900	28.5689	18.58%	55.5600	41.9000	24.59%
2.5	32.1000	19.2100	40.16%	8.1200	3.2954	59.42%	32.1000	19.2300	40.09%
5	18.3700	9.9200	46.00%	1.7000	0.4640	72.71%	18.3700	9.8700	46.27%
7.5	12.7400	6.6300	47.96%	0.6100	0.1431	76.54%	12.7400	6.6400	47.88%
10	9.7200	5.0100	48.46%	0.2800	0.0609	78.25%	9.7200	4.9800	48.77%

TABLE II
COMPARISON OF EXPONENTIAL t_p TIMER AND FIXED t_p TIMER ON $E[t_c]$

	Scheme I (Unit:$1/\mu_m$)			**Scheme II** (Unit:$1/\mu_m$)			**Scheme III** (Unit:$1/\mu_m$)		
λ (Unit: μ_m)	Exponential t_p	Fixed t_p	I_c	Exponential t_p	Fixed t_p	I_c	Exponential t_p	Fixed t_p	I_c
0.1	10.0000	10.0000	0.00%	10.0493	10.0000	0.49%	10.7561	10.0000	7.03%
0.25	4.0000	4.0000	0.00%	4.1196	4.0009	2.88%	4.7647	4.0070	15.90%
0.5	2.0000	2.0000	0.00%	2.2249	2.0344	8.56%	2.7778	2.1165	23.81%
0.75	1.3333	1.3333	0.00%	1.6480	1.4501	12.01%	2.1228	1.5924	24.99%
1	1.0000	1.0000	0.00%	1.3902	1.2179	12.39%	1.8000	1.3712	23.82%
2.5	0.4000	0.4000	0.00%	1.0526	1.0111	3.95%	1.2462	1.0781	13.49%
5	0.2000	0.2000	0.00%	1.0076	0.9996	0.80%	1.0889	1.0234	6.02%
7.5	0.1333	0.1333	0.00%	1.0021	1.0004	0.17%	1.0464	1.0097	3.51%
10	0.1000	0.1000	0.00%	1.0008	0.9994	0.14%	1.0286	1.0067	2.13%

exponential t_p; that is

$$I_\alpha = \frac{\alpha(\text{exponential}) - \alpha(\text{fixed})}{\alpha(\text{exponential})} \tag{32}$$

The larger the I_α, the better the fixed t_p as compared with the exponential t_p. Another indicator I_c represents the percentage of checkpoint interval reduced by fixed t_p over exponential t_p. That is, I_c is defined as

$$I_c = \frac{E[t_c](\text{exponential}) - E[t_c](\text{fixed})}{E[t_c](\text{exponential})} \tag{33}$$

The larger the I_c, the better the exponential t_p as compared with the fixed t_p.

Tables I and II list the output measures α and $E[t_c]$ against λ for both exponential t_p timer and fixed t_p timer. Table I shows that $I_\alpha > 0$ in most cases; that is, the fixed t_p timer often outperforms the exponential t_p timer in terms of α. For example, when $\lambda = \mu_m$, fixed t_p timer outperforms exponential t_p timer by 24.62% in Scheme I, 18.58% in Scheme II and 24.59% in Scheme III. On the other hand, Table II shows that $I_c > 0$ in most cases; that is, the exponential t_p timer often outperforms the fixed t_p timer in term of $E[t_c]$. For example, when $\lambda = \mu_m$, exponential t_p timer outperforms fixed t_p timer by 12.39% in Scheme II and 23.82% in Scheme III. Note that the expected checkpoint interval $E[t_c]$ for Scheme I is not affected by the t_p distribution.

Effects of variance on t_m. We use the discrete event simulation model to investigate the performance of checkpoint schemes with Gamma distributions. The 2-Erlang t_m distribution is a special case of the Gamma distribution. It has been shown that the distribution of any positive random variable can be approximated by a mixture of Gamma distributions (see Lemma 3.9 in [6]). One may also measure time periods in a real mobile network, and the measured data can be approximated by a Gamma distribution. It suffices to use the Gamma distribution with different shape and scale parameters to represent different t_m distributions. For the exponential t_p timer, Fig. 6 plots the output measures α and $E[t_c]$ against the variance V_m of the Gamma inter-registration times. When V_m is very large (i.e. $V_m = 10^2/{\mu_m}^2$), both Schemes II and III have similar α performance. In this case, Scheme III outperforms Scheme II in term of $E[t_c]$. On the other hand, when V_m is very small (i.e., $V_m = 10^{-2}/{\mu_m}^2$), both Schemes II and III have similar $E[t_c]$ performance. In this case, Scheme II outperforms Scheme III in term of α. Therefore, it is appropriate to select Scheme II when the variance V_m of t_m is large. On the other hand, Scheme III should be selected when V_m is small.

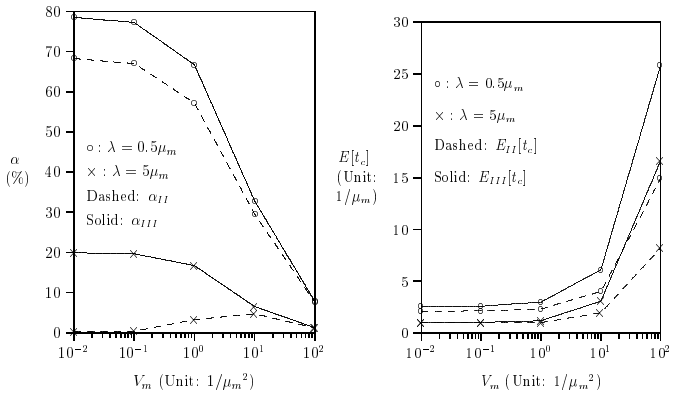

Fig. 6. Effects of V_m on α and $E[t_c]$ (exponential t_p).

VI. Conclusions

We studied checkpointing and failure restoration of Home Location Register (HLR) for UMTS and GPRS. By utilizing per-user checkpoint scheme, an HLR record is saved into a backup database from time to time. When a failure occurs, the backup record is restored to the HLR. We first described a commonly used checkpoint Scheme (referred to as Scheme I). Then we proposed two new checkpoint schemes called Schemes II and III, respectively. An analytic model is developed to compare these three schemes. The output measures considered are the probability α of obsolete HLR backup record and the expected checkpoint interval $E[t_c]$. The analytic model was validated against simulation experiments. We make the following observations.

- Both Schemes II and III are better than Scheme I in terms of the α and the $E[t_c]$ performance. Scheme II is always better than Scheme III in terms of α, and Scheme III is always better than Scheme II in terms of $E[t_c]$.
- The fixed t_p timer often outperforms the exponential t_p timer in term of α. On the other hand, the exponential t_p timer outperforms the fixed t_p timer in term of $E[t_c]$.
- When the variance V_m of the inter-registration times is very large, both Schemes II and III have similar α performance, and Scheme III outperforms Scheme II in term of $E[t_c]$. On the other hand, when V_m is very small, both Schemes II and III have similar $E[t_c]$ performance, and Scheme II outperforms Scheme III in term of α. Therefore, it is appropriate to select Scheme II when the variance V_m is large, and Scheme III should be selected when V_m is small.

As a final remark, we note that failure restoration issues also exist for mobility databases in SGSN and Visitor Location Register. However, the failure restoration solutions for them are very different from that for the HLR. The reader is referred to [5] for the details.

Acknowledgment

This work was sponsored in part by NSC Excellence project NSC 94-2752-E-009-005-PAE, NSC 94-2219-E-009-001, NSC 94-2213-E-009-104, NTP VoIP Project under grant number NSC 94-2219-E-009-002, IIS/Academia Sinica, and ITRI/NCTU Joint Research Center.

References

[1] 3GPP, 3rd Generation Partnership Project, Technical Specification Group Core Network; Restoration procedures (Release 6), Technical Specification 3G TS 23.007 version 6.0.0 (2004-03).

[2] 3GPP, 3rd Generation Partnership Project; Technical Specification Group Services and Systems Aspects; General Packet Radio Service (GPRS); Service Description; Stage 2 (Release 6), Technical Specification 3G TS 23.060 version 6.4.0 (2004-03).

[3] Y. Fang, I. Chlamtac, and H. Fei, "Analytical results for optimal choice of location update interval for mobility database failure restoration in PCS networks," *IEEE Trans. Parallel Distrib. Syst.*, vol. 11, no. 6, pp. 615–624, 2000.

[4] Y. Fang, I. Chlamtac, and H. Fei, "Failure recovery of HLR mobility databases and parameter optimization for PCS networks," *J. Parallel Distrib. Comput.*, vol. 60, pp. 431–450, 2000.

[5] Z. Haas and Y.-B. Lin, "On optimizing the location update costs in the presence of database failures," *ACM/Baltzer Wireless Networks Journal*, vol. 4, pp. 5, pp. 419–426, 1998.

[6] F. P. Kelly, *Reversibility and Stochastic Networks*. John Wiley & Sons, 1979.

[7] Y.-B. Lin, "Per-user checkpointing for mobility database failure restoration," *IEEE Trans. Mobile Comput.*, vol. 4, no. 2, pp. 189–194, 2005.

[8] Y.-B. Lin and Y.-K. Chen, "Reducing authentication signaling traffic in third generation mobile network," *IEEE Trans. Wireless Commun.*, vol. 2, no. 3, pp. 493–504, 2003.

[9] Y.-B. Lin and I. Chlamtac, *Wireless and Mobile Network Architectures*. John Wiley & Sons, 2001.

[10] I. Mitrani, *Modeling of Computer and Communication Systems*. Cambridge University Press, 1987.

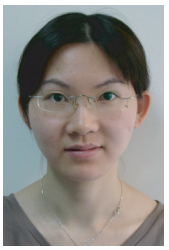

Sok-Ian Sou received the B.S.CSIE. and M.S.CSIE degrees from National Chiao Tung University (NCTU), Taiwan, in 1997 and 2004, respectively. She is currently working toward the Ph.D. degree at NCTU. Her current research interests include personal communications services network, Voice over IP technology and performance modeling.

Yi-Bing Lin (M'96-SM'96-F'03) is Chair Professor and Vice President of Research and Development, National Chiao Tung University. His current research interests include wireless communications and mobile computing. Dr. Lin has published over 190 journal articles and more than 200 conference papers. Lin is the co-author of the book *Wireless and Mobile Network Architecture* (with Imrich Chlamtac; published by John Wiley & Sons). Lin is an IEEE Fellow, an ACM Fellow, an AAAS Fellow, and an IEE Fellow.